Available online at www.sciencedirect.com

ScienceDirect

Biomedical Journal

journal homepage: www.elsevier.com/locate/bj

Original Article

MicroRNA-95-3p inhibits cell proliferation and metastasis in colorectal carcinoma by HDGF

Yong-gang Hong [a,1], Zhi-ping Huang [c,b,1], Qi-zhi Liu [a,1], Ji-Fu E [a,1], Xian-hua Gao [a], Cheng Xin [a], Wei Zhang [a,*], Pengpeng Li [c], Li-qiang Hao [a,*]

[a] Department of Colorectal Surgery, Changhai Hospital, Second Military Medical University, Shanghai, China
[c] The Third Department of Hepatic Surgery, Eastern Hepatobiliary Surgery Hospital, Second Military Medical University, Shanghai, China
[b] The General Hospital of Guangzhou Military Command, Guangzhou, China

ARTICLE INFO

Article history:
Received 20 September 2018
Accepted 11 March 2019
Available online 14 May 2020

Keywords:
MicroRNA-95-3p
HDGF
Colorectal carcinoma
Biomarker
Prognosis

ABSTRACT

Background: MicroRNAs (miRNAs) play an important regulatory role in carcinogenesis and cancer progression. MiR-95-3p has been reported to be an oncogene in hepatocellular carcinoma. However, the role of miR-95-3p in colorectal carcinoma (CRC) remains unclear.
Methods: miR-95-3p was validated in an independent validation sample cohort of 215 CRC tissues. Functional assays, Cell proliferation (MTT) assay colony formation, wound healing, transwell and animal xenograft assays were used to determine the oppressor role of miR-95-3p in human CRC progression. Furthermore, Bioinformatics analysis, western blotting and dual-luciferase reporter assay were used to determine the mechanism by which miR-95-3p suppresses progression of CRC cells.
Results: In this study, we found that miR-95-3p was downregulated in CRC tissues. The low level of miR-95-3p in CRC tumors was correlated with aggressive clinicopathological characteristics, and it predicted poor prognosis in CRC patients. The overexpression of miR-95-3p significantly inhibited CRC cell proliferation, colony formation and metastasis *in vitro* and *in vivo*. Bioinformatic analysis further identified hepatoma-derived growth factor (HDGF) as a novel target of miR-95-3p in CRC cells. These findings suggest that miR-95-3p regulates CRC cell survival, partially through the downregulation of HDGF.
Conclusions: Therefore, the miR-95-3p/HDGF axis might serve as a novel therapeutic target in patients with CRC.

Colorectal cancer (CRC) is the third most common cancer, and it is the fourth leading cause of cancer-related deaths in the world [1,2]. Between one million and two million new cases of CRC are diagnosed each year, and more than 700 000 people die each year [3,4]. Local recurrence and distant metastasis are the main causes leading to death from CRC [5]. Therefore,

* *Corresponding author*. Department of Colorectal Surgery, Changhai Hospital, Second Military Medical University, 168 Changhai Rd, Shanghai, 200433, China
E-mail addresses: weizhang2000cn@163.com (W. Zhang), hao_liqiang@139.com (L.-q. Hao).
Peer review under responsibility of Chang Gung University.
[1] These authors contributed equally to this work.
https://doi.org/10.1016/j.bj.2019.03.006

At a glance of commentary:

Scientific background on the subject

MicroRNAs play an important regulatory role in carcinogenesis and cancer progression. MiR-95-3p has been reported to be an oncogene in hepatocellular carcinoma. However, the role of miR-95-3p in colorectal carcinoma (CRC) remains unclear.

What this study adds to the field

We found that miR-95-3p was downregulated in CRC tissues. The low level of miR-95-3p in CRC tumors was correlated with aggressive clinicopathological characteristics, and it predicted poor prognosis in CRC patients. The overexpression of miR-95-3p significantly inhibited CRC cell proliferation, colony formation and metastasis. Bioinformatic analysis further identified hepatoma-derived growth factor as a novel target of miR-95-3p in CRC cells.

understanding the factors involved in CRC metastasis is necessary for identifying new biomarkers and developing new anticancer strategies.

MicroRNAs (miRNAs or miRs) are small noncoding RNA molecules of 21–25 nucleotides in length that recognize specific complementary sequences that are predominantly located in the 3′-untranslated region (UTR) of target mRNAs and function to either repress translation or degrade target mRNAs [6,7]. Increasing evidence in recent years indicates that many microRNAs play critical roles in oncogenes or tumor suppressors in human cancer [8–13]. Previous studies have shown that miR-95-3p is of great interest for cancer therapies due to its association with various types of cancer [14,15]. The results of functional research on miR-95 seem to be contradictory, as miR-95 promotes the growth of pancreatic, prostate and breast cancer [16,17], while has anticancer activity in hepatic, brain and neck cancer [18,19]. However, miR-95-3p has not been previously reported in CRC. So here we recruited miR-95-3p as a candidate to explore its biological function in CRC.

Materials and methods

Tissue samples

A total of 215 pairs of snap-frozen CRC and peritumoral tissues were obtained from the Changhai Hospital (Shanghai, China). These tissues were used for the quantitative real-time polymerase chain reaction (qRT-PCR) analysis. Micrometastases were defined as tumors adjacent to the border of the main tumor, as observed using a microscope. Tumor staging was defined based on the sixth edition of the Tumor Node Metastasis (TNM) classification system published by the International Union Against Cancer. The tissue samples were stored at −80 °C until further use. The study was approved by the Institutional Review Board of the Changhai Hospital. All patients gave their written informed consent to participate in the study. The data do not contain any information that could identify the patients.

Cell culture

The normal human colon mucosal epithelial cell line NCM460 and the CRC cell lines LS174T, DLD1, HT29, HCT116, SW480, and SW620 were purchased from the Shanghai Institute of Life Sciences Cell Resource Center in Shanghai, China. All cell lines were cultured in DMEM (HyClone) supplemented with 10% fetal bovine serum (FBS) and 1% penicillin/streptomycin (Gibco). All cell cultures were maintained at 37 °C in a humidified atmosphere with 5% CO_2.

Bioinformatic methods

The miRNA targets were predicted using a computer-aided algorithm from TargetScan (http://www.targetscan.org).

Quantitative real-time polymerase chain reaction (qRT-PCR)

Mature miR-95-3p expression was detected using a miRNA-assay kit (Applied Biosystems, Foster City, CA, USA) according to the manufacturer's instructions. The U6 gene was used as a normalization control. All experiments were performed in triplicate and repeated once. To verify the integrity of HDGF expression, the GAPDH gene was used as an internal control. qRT-PCR was run using the following conditions: 30 cycles consisting of denaturation at 94 °C for 30 s, annealing at 56 °C (58 °C for GAPDH) for 30 s, and extension at 72 °C for 30 s. The primer sequences were as follows:miR-195 forward, 5′-ACACTCCAGCTGGGTTCAACGGGTATTTAT-3′ andreverse,5′-TGGTGTCGTGGA GGAGTCG-3'; U6 forward, 5′-CTC GCT TCG GCA GCA CA-3′ and reverse,5′-AACGCTTCA CGA ATT TGC GT-3'; HDGF forward, 5′-GAG GGT GAC GGT GAT AAG AA-3′ and reverse, 5′-GAAACATTGGTG GCTACA GG-3'; and GAPDH forward, 5′-TGCACC ACC AAC TGC TTA GC-3′ and reverse, 5′-GGC ATG CACTGTGGTCATGAG-3'. All samples were amplified in triplicate.

Western blotting assay

Cell lysates were separated using 10% sodium dodecyl sulfate-polyacrylamide gels, electrophoretically transferred to polyvinylidene difluoride membranes (Roche Diagnostics, Mannheim, Germany), and then detected using a mouse anti-HDGF monoclonal (1:500, ab58644, Abcam, USA). Protein loading was estimated using a mouse anti-GAPDH monoclonal (1:1000, ab8245, Abcam, USA)antibody. LabWorks Image Acquisition and Analysis Software (UVP, Upland, CA, USA) were used to quantify the b and intensities.

Luciferase activity assay

The 3′UTR of HDGF was amplified and cloned downstream of the pGL3/luciferase (Luc) vector. The mutant 3′UTR of HDGF (several nucleotides within the binding sites were mutated)

was amplified using the pGL3/Luc-HDGF 3′UTR as the template and then cloned downstream of the pGL3/Luc vector. For the luciferase reporter assay, the cells were cotransfected with either miR-95-3p mimics or control and the pGL3/Luc-HDGF 3′UTR or the mutant 3′UTR, together with the controls. Then, 48 h after transfection, the cells were lysed using RIPA buffer, and luciferase intensity was measured using an F-4500 Fluorescence Spectrophotometer (HIT-ACHI).

Transfection

For stable transfection, the lentiviral expression vectors LV-Control and LV-HDGF were obtained from Shanghai Gene Pharma Company (China). Lentiviruses were mixed with polybrene (5 mg/ml), and HCT116 cells were added. Positive clones were selected in puromycin (5 mg/ml). Stable HDGF transfectants were isolated after 2 weeks.

Cell proliferation (MTT) assay and colony formation assay

The transfected cells were plated onto 96-well plates at a density of 5000 cells/well. Then, 48 h after transfection, the cells were incubated with MTT (3-(4, 5-dimethylthiazol-2-yl)-2, 5-diphenyltetrazolium bromide) for 4 h at 37 °C. The cells were then agitated with MTT solvent on an orbital shaker for 10 min while avoiding light. The absorbance was

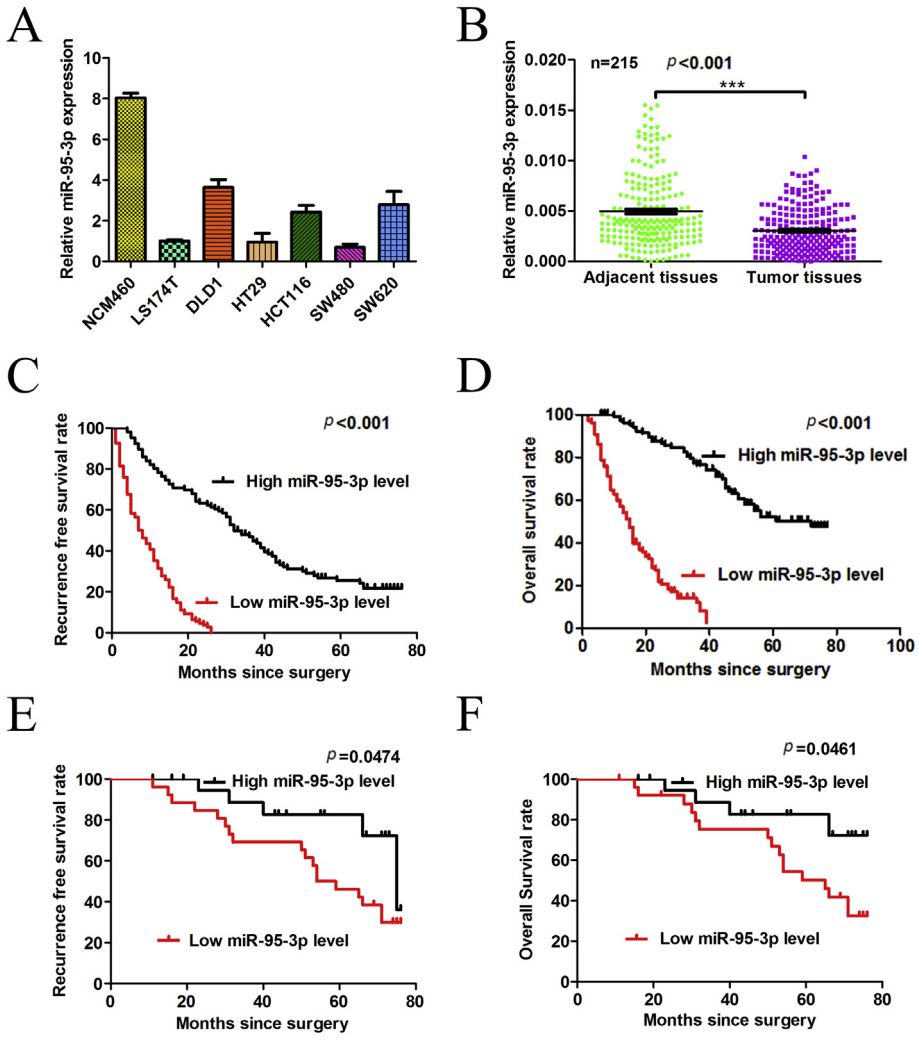

Fig. 1 MiR-95-3p expression is downregulated in human CRC. (**A**)The expression of miR-95-3p was significantly lower in CRC cell lines than in normal liver cells. MiR-95-3p expression was normalized to U6 expression. (**B**)The relative expression of miR-95-3p was analyzed in 215 cases of CRC using qRT-PCR and was normalized to U6 expression. (**C**) The low miR-95-3p expression group showed a shorter RFS than the high miR-95-3p expression group. (**D**) The low miR-95-3p expression group showed a shorter OS than the high miR-95-3p expression group. (**E** and **F**) The prognostic value of miR-95-3p was also observed in patients with early-stage CRC (TNM stage I). Statistical significance was assessed by two-sided log-rank tests. (*$p < 0.05$; *$p < 0.005$; ***$p < 0.001$).

measured at 450 nm (OD450 nm) using a spectrophotometer. The transfected cells were seeded onto 12-well plates at a density of 200 cells/well. The medium was changed every 3 days. Approximately 10 days after seeding, most of the cell clones contained more than 50 cells. The clones were washed with 1 × PBS and stained with crystal violet for approximately 5 min. The clones were imaged and counted, and the colony formation rate was calculated using the following formula (number of clones)/(number of seeded cells) × 100%.

Transwell assays

Millicell 24-well culture insert plates (Millipore, USA) and polycarbonate membranes with a pore size of 8 μm were used in the transwell assays as follows. First, the insert plates were equilibrated with 0.5 ml of DMEM for 1 h at 37 °C with 5% CO_2. The medium was then replaced with 0.5 ml of DMEM supplemented with 10% FBS in the lower chambers. In total, 50 000 cells in 400 μL of serum-free DMEM were loaded into the upper chambers. After 24 h of incubation, the insert plates were rinsed with PBS, and the upper surfaces of the membranes were scraped to remove the cells. The cells on the underside of the membrane were stained with Giemsa stain and counted using a microscope. Cells from each culture condition were examined in quadruplicate.

Wound healing assays

For the wound healing assays, a monolayer of cells plated onto 12-well plates was wounded by scraping the monolayer with a 200-μL plastic pipette tip. The cells were then rinsed several times with medium to remove any floating cells. The wound healing process was monitored with an inverted light microscope (Olympus).

Animal studies

The animal studies were approved by the Institutional Animal Care and Use Committee of the Second Military Medical University in Shanghai, China. To explore the effects of miR-95-3p on tumor growth *in vivo*, 1×10^7 HCT116 cells, which stably overexpressed miR-95-3p, or control cells were subcutaneously implanted into the bilateral armpit of nine BALB/c nude mice. The tumor volume was measured each week following implantation (volume, V = length × width × height × 1/2). All mice were sacrificed 5 weeks later. Eighteen 6-week-old male nude mice were assigned randomly into two groups, and the cells (4×10^5) were injected into the tail vein of the mice to establish a pulmonary metastatic model. The mice were sacrificed 10 weeks after the injection and microscopically examined for the development of lung metastatic foci via H & E staining. The animals were housed in cages under standard pathogen-free conditions, in accordance with the requirements of the Second Military Medical University Animal Care Facility and the National Institutes of Health guidelines.

Statistical analysis

Statistical analyses were performed using SPSS version 23.0(IBM).

Student's t-test was adopted to determine statistical differences between two groups. One-way ANOVA was adopted to determine statistical differences between multiple tests. The chi-square test was used to analyze the relationship between miR-95-3p expression and clinicopathological characteristics. Survival curves were plotted by the Kaplan Meier method and compared by log-rank test. Multivariate analyses were performed using the Cox multivariate proportional hazard regression model in a stepwise manner (forward, likelihood ratio). $p < 0.05$ was considered significant. All the experiments were repeated three times.

Table 1 Clinical characteristics of 215 CRC patients according to the miR-95-3p expression levels.

Feature	miR-95-3p		*p*-value*
	High # (n = 107)	Low # (n = 108)	
All cases			
Age, y			0.637
≥60	48	44	
<60	59	64	
Sex			0.251
Male	93	100	
Female	14	8	
CEA, μg/L			0.017
≥5	45	64	
<5	62	44	
Tumor location			0.048
Rectum	57	42	
Colon	50	66	
Differentiation grade			0.634
Moderate + Poor	65	70	
Well	42	38	
Tumor size, cm			<0.001
≥5	51	83	
<5	56	25	
Local invasion			<0.001
pT_3-pT_4	15	56	
pT_1-pT_2	92	52	
Lymph node metastasis			0.374
Positive	59	52	
Negative	48	56	
Adjuvant chemotherapy			<0.001
Present	83	54	
Absent	24	54	
TNM stage			<0.001
III-IV	43	82	
I-II	64	26	

#The median expression level was used as the cutoff. Low miR-95-3p expression in each of the 108 patients was defined as a value below the 50th percentile. High miR-95-3p expression in each of the 107 patients was defined as a value above the 50th percentile.
*For analysis of correlation between the expression levels of miR-95-3p and the clinical features, Pearson chi-square tests were used. The results were considered statistically significant at $p < 0.05$.

Results

MiR-95-3p expression is downregulated in human CRC

To explore the role of miR-95-3p in CRC, we first examined the expression of miR-95-3p in CRC cell lines. As shown in Fig. 1A, miR-95-3p expression was lower in CRC cell lines than in NCM460 cells. We then detected the expression of miR-95-3p in a total of 215 matched CRC tumor tissues and their corresponding adjacent nontumor samples. Our results indicated that miR-95-3p was significantly lower in tumor tissues than in nontumor tissues [Fig. 1B]. Therefore, we speculated that the downregulation of miR-95-3p expression might play an important role in CRC progression and development.

Decreased miR-95-3p expression predicts aggressive clinicopathological characteristics and poor prognosis in CRC patients

To investigate the clinical significance of miR-95-3p in CRC, the cohort of 215 CRC patients was divided into two groups: a low miR-95-3p expression (below the median expression level, n = 108) group and a high miR-95-3p expression (above the median expression level, n = 107) group. We found that low miR-95-3p expression was associated with tumor location ($p = 0.048$), larger tumor size (≥5 cm) ($p < 0.001$), local invasion ($p < 0.001$), adjuvant chemotherapy use ($p < 0.001$), advanced TNM stage ($p < 0.001$)and high CEA serum levels ($p = 0.017$) [Table 1]. Kaplan–Meier survival analysis showed that CRC patients in the low miR-95-3p expression group exhibited worse recurrence survival (RFS) and overall survival (OS) than patients in the high miR-95-3p expression group ($p < 0.0001$; $p < 0.0001$, respectively) [Fig. 1C, D]. The prognosis of some patients with early-stage CRC remains poor, suggesting that a supplementary prognostic predictor is required for these patients. Therefore, patients with early-stage CRC (TNM stage I) were stratified, and subgroup analyses were performed. Notably, the prognosis-predictive value of low miR-95-3p expression in early-stage CRC (TNM stage I) was still proven (RFS, $p = 0.0474$ and OS, $p = 0.0461$) [Fig. 1E, F]. A univariate analysis indicated that among the clinicopathological characteristics, miR-95-3p expression level, tumor location, larger tumor size, local invasion, adjuvant chemotherapy, TNM stage, and CEA positivity were correlated with RFS and OS [Table 2]. Furthermore, multivariate Cox regression analysis indicated that the miR-95-3p expression level, CEA positivity, larger tumor size, adjuvant chemotherapy, and TNM stage were independent risk factors for RFS and that the miR-95-3p expression level, CEA positivity, larger tumor size, local invasion, adjuvant chemotherapy, and TNM stage were independent risk factors for OS in CRC patients [Table 3]. Taken together, these results indicate that miR-95-3p may represent a valuable prognostic biomarker for CRC.

Overexpression of miR-95-3p inhibits CRC cell proliferation in vitro and in vivo

To determine the effect of miR-95-3p on CRC cell behavior, we overexpressed miR-95-3p in the HCT116 and SW620 cell lines [Fig. 2A]. To confirm that miR-95-3p could function as a tumor suppressor, the effects of miR-95-3p overexpression on CRC cell proliferation were determined *in vitro*. As shown in Fig. 2B, C, the overexpression of miR-95-3p inhibited CRC cell proliferation. In parallel, HCT116 and SW620 cells that overexpressed miR-95-3p formed fewer colonies than control cells [Fig. 2D, E]. To determine the effects of miR-95-3p on

Table 2 Univariable analysis for RFS (recurrence survival) and OS (overall survival).

Variable	RFS			OS		
	Hazard Ratio	95% CI	p *value*	Hazard Ratio	95% CI	p *value*
Age, y						
≥60 vs. <60	0.794	0.593–1.062	0.120	0.842	0.599–1.183	0.322
Sex						
male vs. female	1.232	0.766–1.983	0.389	1.049	0.613–1.794	0.862
CEA, ug/L						
≥5 vs.<5	2.470	1.823–3.346	<0.001	2.737	1.922–3.896	<0.001
Tumor location						
Rectum vs. Colon	1.503	1.127–2.005	0.006	1.952	1.393–2.736	<0.001
Differentiation grade						
Moderate + Poor vs. Well	0.810	0.603–1.087	0.161	0.995	0.699–1.414	0.976
Tumor size, cm						
≥5 vs. <5	3.021	2.189–4.169	<0.001	3.055	2.082–4.484	<0.001
Local invasion						
PT_3-PT_4 vs. PT_1-PT_2	3.118	2.273–4.277	<0.001	3.78	2.607–5.479	<0.001
Lymph node metastasis						
Positive vs. Negative	1.178	0.884–1.572	0.264	1.231	0.88–1.724	0.225
Adjuvant chemotherapy						
Absent vs. Present	2.983	2.155–4.128	<0.001	2.768	1.882–4.07	<0.001
TNM stage						
III-IV vs. I-II	2.156	1.524–2.971	<0.001	2.645	1.846–3.92	<0.001
miR-95-3p expression						
low vs. high	7.052	4.785–10.395	<0.001	10.322	6.448–16.523	<0.001

Table 3 Multivariable analysis of RFS (recurrence survival) and OS (overall survival) in patients with CRC.

Variable	RFS			OS		
	Hazard Ratio	95% CI	p *value*	Hazard Ratio	95% CI	p *value*
CEA, μg/L						
≥5 vs.<5	2.362	1.735–3.253	<0.001	2.677	1.823–3.899	<0.001
Tumor location						
Rectum vs. Colon	0.973	0.728–1.355	0.833	1.288	0.841–1.842	0.162
Tumor size, cm						
≥5 vs. <5	2.330	1.644–3.227	<0.001	2.171	1.434–3.266	<0.001
Local invasion						
PT_3-PT_4 vs. PT_1-PT_2	1.321	0.909–1.855	0.143	1.549	1.022–2.365	0.041
Adjuvant chemotherapy						
Absent vs. Present	1.833	1.268–2.610	0.001	1.822	1.193–2.781	0.006
TNM stage						
III-IV vs. I-II	1.389	1.010–1.864	0.027	1.615	1.156–2.337	0.006
miR-95-3p expression						
low vs. high	4.274	2.722–6.688	<0.001	16.848	3.947–11.777	<0.001

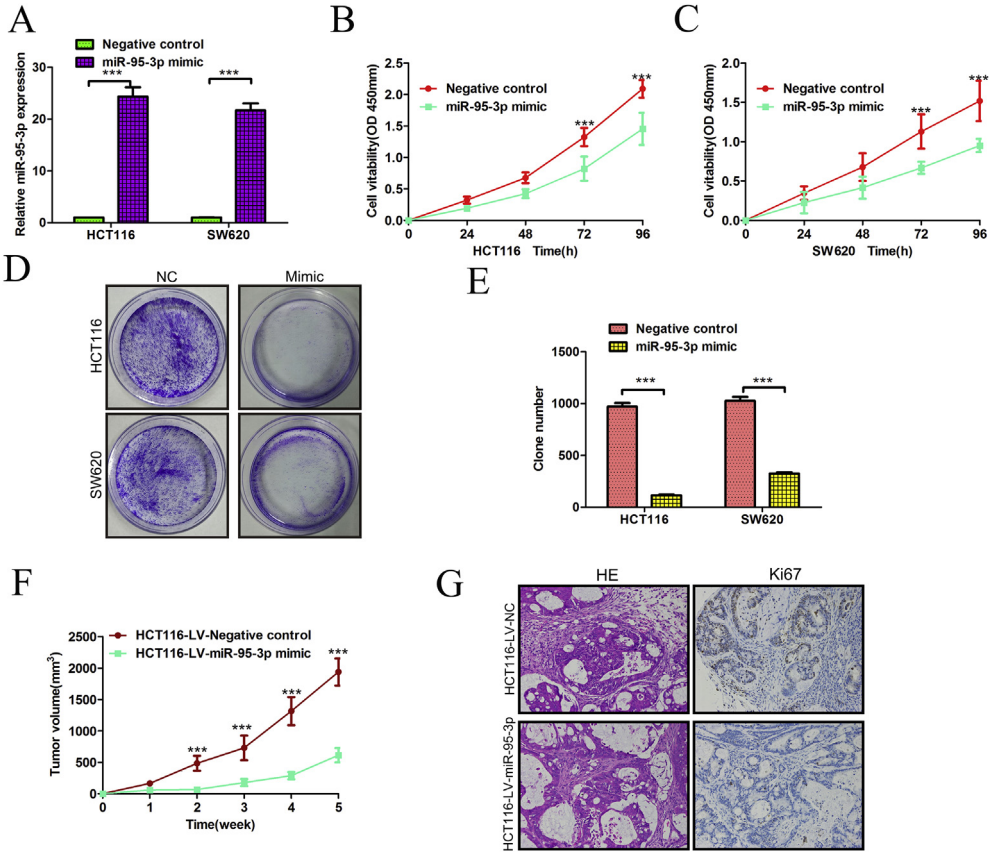

Fig. 2 Overexpression of miR-95-3p inhibits CRC cell growth *in vitro and in vivo*. (**A**) Overexpression of miR-95-3p in HCT116 and SW620 cells was assessed using qRT-PCR. MiR-95-3p expression was normalized to U6 expression. (**B,C**) MTT assays were performed 24 h, 48 h, 72 h and 96 h after transfection to determine the proliferation of HCT116 and SW620 cells. The data represent the mean ± SD from three independent experiments. (**D,E**) Colony formation assays were performed in HCT116 and SW620 cells transfected with miR-95-3p mimics or a negative control. The average number of colonies and representative images are shown. (**F**) Tumor growth in xenografted mice 5 weeks after subcutaneous injection with either miR-95-3p or miR-GFP cells (n = 9). (**G**) The indicated xenograft tumors were subjected to immunohistochemical staining of Ki67. Representative images are shown in the left panel (magnification, × 200). (*$p < 0.05$; *$p < 0.005$; ***$p < 0.001$).

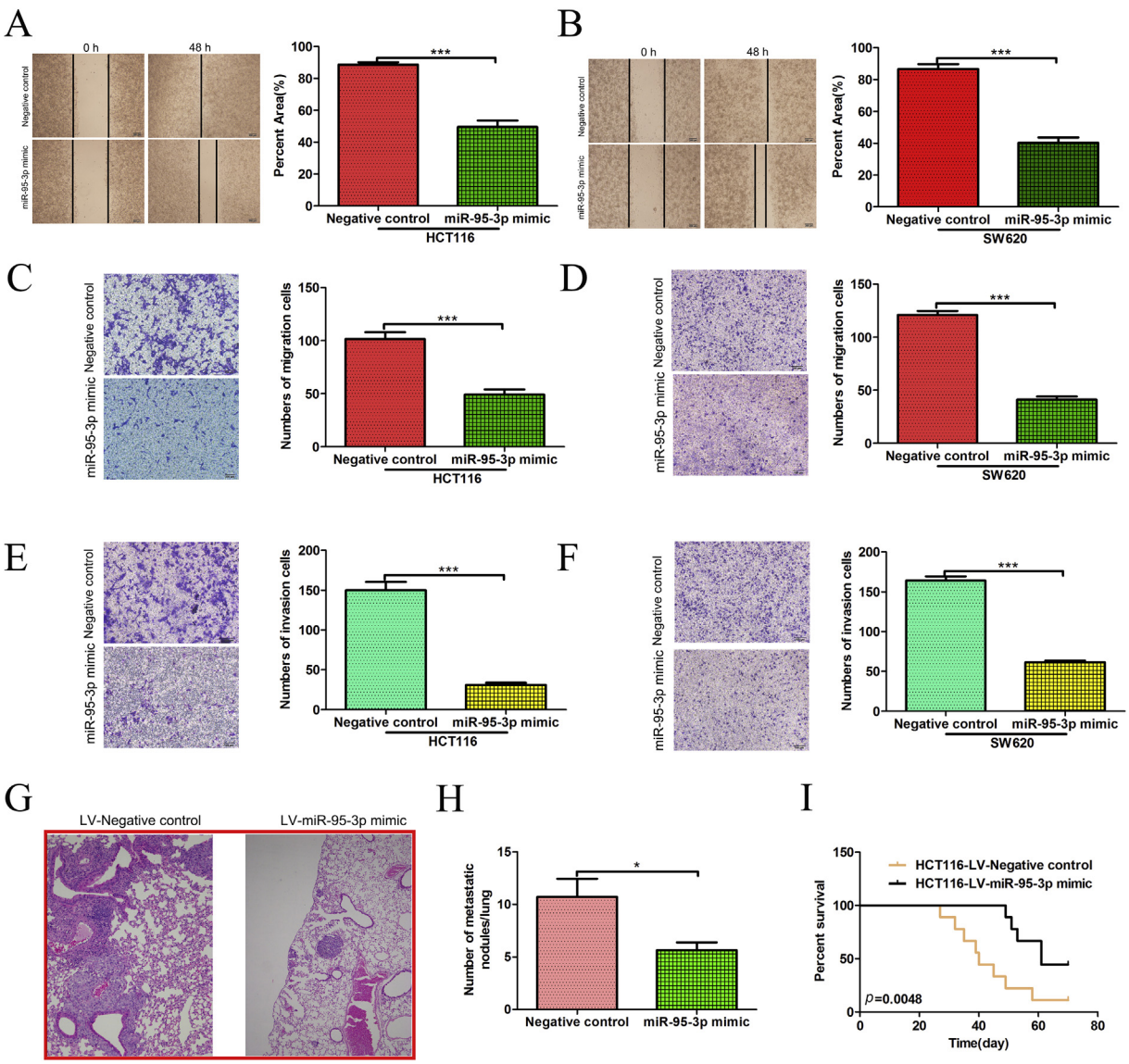

Fig. 3 Overexpression of miR-95-3p inhibits CRC cell metastasis *in vitro* and *in vivo*. (**A,B**) The migratory properties of miR-95-3p-overexpressing cells and control cells were analyzed by scratch wound healing assays in HCT116 and SW620 cells. Representative results are shown. Magnification: ×100(**C,D**) The migratory properties of the cells were analyzed using the Transwell migration assay with Transwell filter chambers. The results are plotted as the average number of migrated cells from 6 random microscopic fields. (**E,F**) The invasive properties of the cells were analyzed with an invasion assay using BioCoat Matrigel invasion chambers. The results are plotted as the average number of invasive cells from 6 random microscopic fields. (**G**) Representative H & E images of mouse lung tissue sections from the LV-miR-95-3p mimic and LV-Negative control groups (magnification: ×200). (**H**)The number of metastatic foci in the lungs of each group (n = 9) is presented as the mean ± SD (error bars). (**I**)Comparisons of the OS curves of mice injected with either the LV-miR-95-3p mimic or LV-Negative control. *p* values were calculated using the 2-sided log-rank test. (*$p < 0.05$; *$p < 0.005$; ***$p < 0.001$).

tumorigenesis *in vivo*, we subcutaneously injected HCT116 cells that stably overexpressed miR-95-3p or miR-GFP into nude mice for xenograft transplantation. As shown in Fig. 2F, mice injected with miR-95-3p-overexpressing cells showed significantly less tumor growth than mice injected with miR-GFP-transfected cells. In addition, the xenograft tumors were subjected to immunohistochemical staining for proliferating cell nuclear antigen (PCNA), which was used as a proliferation marker. Notably, the number of Ki67-positive nuclei was markedly decreased in the miR-95-3p-overexpressing xenograft tumors compared to that in the control counter parts [Fig. 2G]. Therefore, these results indicated that ectopic miR-95-3p expression inhibited CRC cell proliferation *in vitro* and *in vivo*.

Overexpression of miR-95-3p inhibits CRC cell metastasis in vitro *and* in vivo

Next, we determined the effects of miR-95-3p overexpression on CRC cell metastasis *in vitro*. A wound healing migration

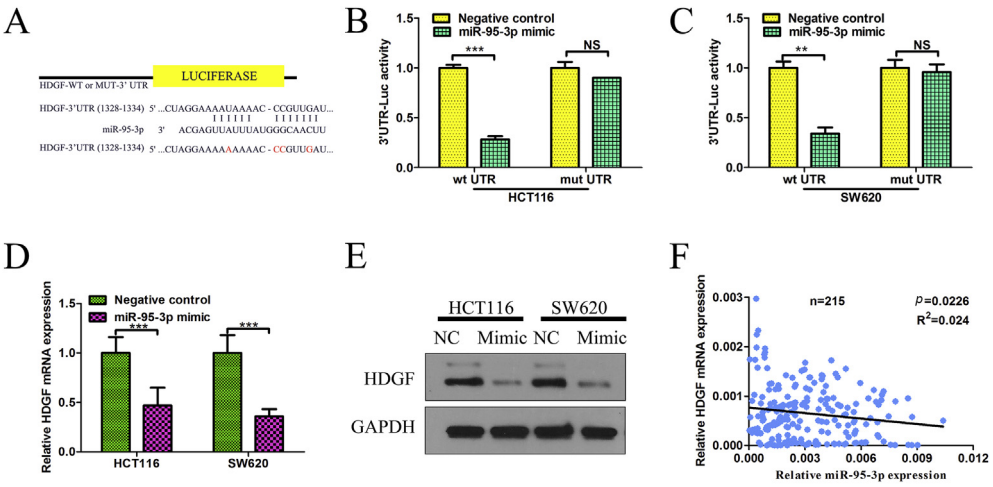

Fig. 4 MiR-95-3p directly targets HDGF. (**A**) The putative miR-95-3 pbinding sites in the 3′UTR of HDGF mRNA are shown. A mutation was generated in the HDGF 3′UTR sequence at the complementary site for the seed sequence of miR-95-3p. (**B**) Wild-type (HDGF 3′UTR-WT) or mutant (HDGF 3′UTR-mut) reporter plasmids were cotransfected into HCT116 cells with miR-95-3p or miR-GFP. The normalized luciferase activity in the control group was set as the relative luciferase activity. (**C**) Wild-type (HDGF 3′UTR-WT) or mutant (IGF 3′UTR-mut) reporter plasmids were cotransfected into SW620 cells with MmiR-95-3p or miR-GFP. The normalized luciferase activity in the control group was set as the relative luciferase activity. (**D**) The mRNA expression of HDGF was analyzed using qRT-PCR in HCT116 and SW620 cells. GAPDH was used as an internal control. (**E**)HDGF protein expression was analyzed using Western blotting in HCT116 and SW620 cells. GAPDH was used as an internal control. (**F**)The correlation between the miR-95-3p level and HDGF mRNA level was measured in the same set of tissues ($^{*}pP < 0.05$; $^{*}p < 0.005$; $^{***}p < 0.001$).

assay showed that miR-95-3p overexpression could inhibit cell migration in HCT116 and SW620 cells [Fig. 3A, B]. Migration and invasion assays with these miR-95-3p-overexpressing cell lines also showed that cell mobility was dramatically decreased in cells with exogenous expression of miR-95-3p compared to that in control cells [Fig. 3C–F]. To verify the *in vivo* consequences of miR-95-3p overexpression, we injected HCT116 cells that stably overexpressed miR-95-3p or miR-GFP cells into the lateral tail vein of nude mice and evaluated both the metastatic growth in the lungs and the survival of the mice. Ten weeks later, the mouse lungs were stained with H & E, and lung micro metastases were microscopically evaluated [Fig. 3G, H]. Fewer and smaller metastatic foci were detected in the mice injected with the HCT116-miR-95-3p cells than in the control mice. In addition, mice injected with HCT116-miR-95-3p cells had a significantly higher survival rate [Fig. 3I].

MiR-95-3p directly targets HDGF

The miRNA target prediction algorithm TargetScan was used to computationally screen for genes with miR-95-3p complementary sites in their 3′UTR. The results showed that HDGF was a putative target of miR-95-3p. The miR-95-3p binding sequences in the 3′UTR of HDGF mRNA (WT-3′UTR) or its mutant (HDGF-3′UTR-mut) were subcloned downstream of the luciferase reporter vector pGL3 [Fig. 4A]. As shown in Fig. 4B, C, the relative luciferase activity of the reporter containing the HDGF WT-3′UTR was significantly decreased when miR-95-3p was cotransfected, whereas the luciferase activity of the HDGF-3′UTR-mut reporter was unaffected in HCT116 and SW620 cells. These results suggest that miR-95-3p might suppress HDGF expression through the putative binding site in its 3′UTR. Furthermore, qRT-PCR and Western blot assays were performed to determine whether miR-95-3p expression affects the expression of endogenous HDGF at both the transcriptional and translational levels. The mRNA levels of HDGF were consistently decreased in miR-95-3p-overexpressing CRC cells [Fig. 4D]. Furthermore, Western blot analysis showed that the expression of HDGF was significantly inhibited following the overexpression of miR-95-3p [Fig. 4E]. Moreover, miR-95-3p levels were negatively correlated with the HDGF transcript levels in the tumor tissues [Fig. 4F]. These data indicated that miR-95-3p inhibited HDGF expression in CRC cells by targeting its 3′UTR.

Rescued expression of HDGF abolishes the effects of miR-95-3p on the phenotypes of CRC cells

To determine if the HDGF gene is required for the effects of miR-95-3p on CRC cell proliferation and metastasis, ectopic overexpression of HDGF was induced to conduct functional studies in HCT116 and SW620 cells [Fig. 5A, B]. Fig. 5C, D shows that the overexpression of HDGF abolished the effects of miR-95-3p on the inhibition of CRC cell proliferation. Furthermore, the capacities of migration and invasion in HDGF-overexpressing CRC cells were significantly enhanced, while the overexpression of HDGF abolished the effects of miR-95-3p on the inhibition of CRC cell migration and invasion ability

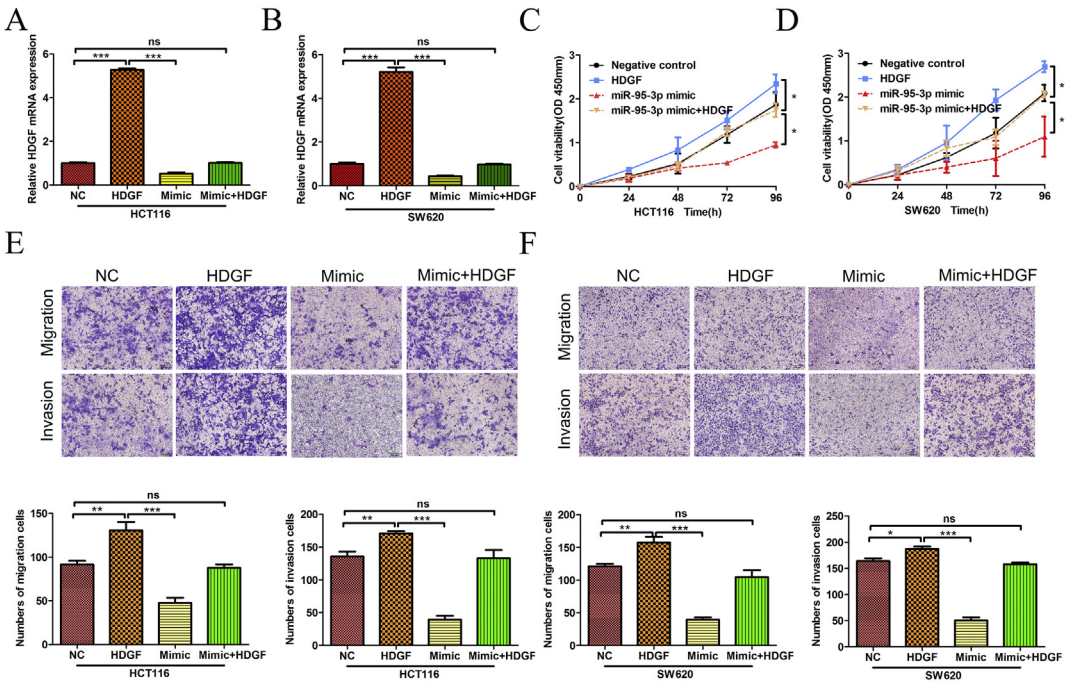

Fig. 5 Rescued expression of HDGF abolishes the effects of miR-95-3p on the phenotypes of CRC cells. (**A**,**B**) The expression levels of HDGF in HCT116 and SW620 cells were examined by qRT-PCR. (**C**,**D**) MTT assays were performed 24 h, 48 h, 72 h and 96 h after transfection to determine the proliferation of HCT116 and SW620 cells. The data represent the mean ± SD from three independent experiments. (**E**,**F**) The migratory properties of the cells were analyzed using the Transwell migration assay with Transwell filter chambers. The results are plotted as the average number of migrated cells from 6 random microscopic fields, and the invasive properties of the cells were analyzed with the invasion assay using BioCoat Matrigel invasion chambers. The results are plotted as the average number of invasive cells from 6 random microscopic fields (*$p < 0.05$; *$p < 0.005$; ***$p < 0.001$).

[Fig. 5E, F]. Therefore, HDGF overexpression abolishes the effects of miR-95-3p on the phenotypes of CRC cells.

Discussion

In this study, we found that miR-95-3p was downregulated in CRC tumor tissues and CRC cell lines. MiR-95-3p downregulation was correlated with poor prognosis. Functionally, the abnormal expression of miR-95-3p has been hypothesized to contribute to the malignant phenotype of several tumors. For example, in hepatocellular carcinoma, the ectopic expression of miR-95-3p promotes tumorigenesis by targeting p21 expression [20]. In our study, the overexpression of miR-95-3p in HCT116 and SW620 cells significantly inhibited cell proliferation and metastasis both *in vitro* and *in vivo*. These results strongly suggest that miR-95-3p plays an inhibitory role in CRC.

Previous studies have demonstrated that serum carcinoembryonic antigen (CEA) is both an important prognostic factor and an indicator of therapeutic effects and recurrence in patients with rectal cancer [21,22]. CEA is produced in normal cells and at a higher level in the presence of certain cancers. The persistent elevation of CEA levels after surgery for colorectal cancer may indicate incomplete resection or occult metastatic disease, and it demonstrates a prognostic feature for relapse [23]. The relationship between the expression of miR-95-3p and serum CEA levels suggests that miR-95-3p may be a potential biomarker in the diagnosis of CRC.

As miR-95-3p has hardly been investigated in CRC previously, we planned functional experiments on multiple aspects of tumorigenesis, including proliferation, clone formation, migration and invasion. In order to set up the experimental group, miR-95-3p mimic was transfected into CRC cells to enhance the miR-95-3p level. In MTT assay, we observed upregulation of miR-95-3p repressed CRC cells proliferation. As migration and invasiveness is important factors in tumor metastasis, we also performed transwell test to investigate the function of miR-95-3p on this aspect. Less cells transfected with miR-95-3p mimic invaded through the membrane than control, as we expected. *In vivo* experiments also indicated that miR-95-3p inhibited tumor growth and metastasis of CRC. These results suggested that miR-95-3p may act as a anticancer factor in CRC.

MicroRNAs can function as tumor suppressors or oncogenes by targeting oncogenes or tumor suppressor genes, respectively. In this study, we explored the miR-95-3p targets that may contribute to its inhibition of cell proliferation and metastasis in CRC. Using TargetScan bioinformatics, we identified the HDGF gene as a possible direct target of miR-95-3p. HDGF, a heparin-binding growth factor, was originally

purified from conditioned culture medium from the hepatoma HuH7 cell line [24]. The HDGF gene is located on chromosome 1, region q21-q23 [25]. Previous studies have demonstrated that the knockdown of HDGF decreased neoplastic transformation and proliferation [25–27]. It has been confirmed that HDGF is involved in the regulation of cell apoptosis, angiogenesis, invasion and metastasis [28]. A number of studies have demonstrated that HDGF is upregulated in various types of human tumors, including gastric cancer, hepatocellular carcinoma, pancreatic cancer and esophageal carcinoma and that HDGF is associated with poor prognosis [29–32]. HDGF was also found to be upregulated and correlated with poor prognosis in cervical adenocarcinoma [33]. HDGF has been identified to be regulated by multiple miRNAs in many types of cancer. For example, in lung cancer, miR-16 and miR-497 negatively regulated HDGF expression to inhibit cell proliferation, invasion and angiogenesis [29,34]. In gastric cancer, miR-141 suppressed cell proliferation, migration and invasion by directly targeting HDGF [35]. In this study, we performed a luciferase reporter assay, qRT-PCR and Western blotting to verify that miR-95-3p can directly target HDGF by interacting with its 3′UTR. To determine whether miR-95-3p regulates CRC cells biological behavior by HDGF, rescue experiments were performed. From the results we found that the effects of miR-95-3p inhibiting CRC proliferation and metastasis were rescued by increased expression of HDGF. Thus, the miR-95-3p-HDGF regulation mechanism on CRC was established. To the best of our knowledge, our study is the first to report that miR-95-3p acts as a tumor suppressor in CRC. In addition, we observed that miR-95-3p expression was negatively correlated with HDGF transcription in CRC. This finding implies that miR-95-3p might act as a tumor suppressor or play a similar role by decreasing HDGF expression. Our results indicate that the miR-95-3p/HDGF axis might serve as a novel therapeutic target in patients with CRC.

Conclusions

In summary, miR-95-3p expression is frequently decreased in CRC tumor tissues and may serve as a prognostic bio-marker in patients with CRC. The overexpression of miR-95-3p inhibited CRC cell proliferation by directly suppressing the expression of HDGF; this finding not only sheds new light on CRC progression and metastasis but also provides a potential target for cancer prevention and treatment.

Conflicts of interest

The authors declare no competing interests.

Acknowledgments

This work was supported by the Natural Science Foundation of the Shanghai Science and Technology Commission (No. 16ZR1400800).

Appendix A. Supplementary data

Supplementary data to this article can be found online at https://doi.org/10.1016/j.bj.2019.03.006.

REFERENCES

[1] Brenner H, Kloor M, Pox CP. Colorectal cancer. Lancet 2014;383:1490–502.
[2] Torre LA, Bray F, Siegel RL, Ferlay J, Lortet-Tieulent J, Jemal A. Global cancer statistics, 2012. CA - Cancer J Clin 2015;65:87–108.
[3] Brody H. Colorectal cancer. Nature 2015;521:S1.
[4] Mármol I, Sánchezdediego C, Dieste AP, Cerrada E. Colorectal carcinoma: a general overview and future perspectives in colorectal cancer. Int J Mol Sci 2017;18:197.
[5] Shi S, Yang J, Sun D. CT-guided (125)I brachytherapy on pulmonary metastases after resection of colorectal cancer: a report of six cases. Oncology Lett 2015;9:375–80.
[6] Moreno JM. MicroRNA: key gene expression regulators - fertility and Sterility. Fertil Steril 2014;101:1516–23.
[7] Vasudevan S, Tong Y, Steitz JA. Switching from repression to activation: MicroRNAs can up-regulate translation. Science 2007;318:1931–4.
[8] Kong YW, Ferland-Mccollough D, Jackson TJ, Bushell M. microRNAs in cancer management. Lancet Oncol 2012;13:e249–58.
[9] Lieb V, Weigelt K, Scheinost L. Serum levels of miR-320 family members are associated with clinical parameters and diagnosis in prostate cancer patients. Oncotarget 2018;9:10402–16.
[10] Mu K, Kayani MA, Malik FA, Faryal R. Role of miRNAs in breast cancer. Asian Pac J Cancer Prev APJCP 2011;12:3175–80.
[11] Song Q, Chen Q, Wang Q, Yang L, Lv D, Jin G, et al. ATF-3/miR-590/GOLPH3 signaling pathway regulates proliferation of breast cancer. BMC Canc 2018;18:255.
[12] Voorhoeve PM, Le SC, Schrier M, Gillis AJ, Stoop H, Nagel R, et al. A genetic screen implicates miRNA-372 and miRNA-373 as oncogenes in testicular germ cell tumors. Cell 2006;124:1169–81.
[13] Zhang B, Pan X, Cobb GP, Anderson TA. RNAs as oncogenes and tumor suppressors. Dev Biol Dev Biol 2007;302:1–12.
[14] Wang YY, Wu ZY, Wang GC, Liu K, Niu XB, Gu S, et al. LINC00312 inhibits the migration and invasion of bladder cancer cells by targeting miR-197-3p. Tumor Biol 2016;37:14553–63.
[15] Fan B, Jiao BH, Fan FS, Lu SK, Song J, Guo CY, et al. Downregulation of miR-95-3p inhibits proliferation, and invasion promoting apoptosis of glioma cells by targeting CELF2. Int J Oncol 2015;47:1025–33.
[16] Xiaoyong H, Samira T, Sahar J, Urban E, Elisa T, Jeff B, et al. miRNA-95 mediates radioresistance in tumors by targeting the sphingolipid phosphatase SGPP1. Cancer Res 2013;73:6972–86.
[17] Zhang Y, Min L, Hao W, Fisher WE, Lin PH, Yao Q, et al. Profiling of 95 MicroRNAs in pancreatic cancer cell lines and surgical specimens by real-time PCR analysis. World J Surg 2009;33:698–709.
[18] Alpha Mu NS, Yoke-Kqueen C,, Sabariah AR, Shiran MS, Singh A, Learn-Han L. Differential microRNA expression and identification of putative miRNA targets and pathways in head and neck cancers. Int J Mol Med 2011;28:327.

[19] Xiao Z, Chow SC, Li CH, Tang SC, Tsui SKW, Lin Z, et al. Role of microRNA-95 in the anticancer activity of Brucein D in hepatocellular carcinoma. Eur J Pharmacol 2014;728:141–50.
[20] Ye J, Yao Y, Song Q, Li S, Hu Z, Yu Y, et al. Up-regulation of miR-95-3p in hepatocellular carcinoma promotes tumorigenesis by targeting p21 expression. Sci Rep 2016;6:34034.
[21] Song S, Hong JC, Mcdonnell SE, Koong AC, Minsky BD, Chang DT, et al. Combined modality therapy for rectal cancer: the relative value of posttreatment versus pretreatment CEA as a prognostic marker for disease recurrence. Ann Surg Oncol 2012;19:2471–6.
[22] Tarantino I, Warschkow R, Schmied BM, Güller U, Mieth M, Cerny T, et al. Predictive value of CEA for survival in stage I rectal cancer: a population-based propensity score-matched analysis. J Gastrointest Surg Off J Soc Surg Aliment Tract 2016;20:1213–22.
[23] Lin JK, Lin CC, Yang SH, Wang HS, Jiang JK, Lan YT, et al. Early postoperative CEA level is a better prognostic indicator than is preoperative CEA level in predicting prognosis of patients with curable colorectal cancer. Int J Colorectal Dis 2011;26:1135–41.
[24] Huang JS, Chao CC, Su TL, Yeh SH, Chen DS, Chen CT, et al. Diverse cellular transformation capability of overexpressed genes in human hepatocellular carcinoma. Biochem Biophys Res Commun 2004;315:950–8.
[25] Zhang J, Ren H, Yuan P, Lang W, Zhang L, Mao L. Down-regulation of hepatoma-derived growth factor inhibits anchorage-independent growth and invasion of non-small cell lung cancer cells. Cancer Res 2006;66:18–23.
[26] Lee KH, Choi EY, Kim MK, Lee SH, Jang BI, Kim TN, et al. Hepatoma-derived growth factor regulates the bad-mediated apoptotic pathway and induction of vascular endothelial growth factor in stomach cancer cells. Oncol Res 2010;19:67–76.
[27] Ren H, Chu Z, Mao L. Antibodies targeting hepatoma-derived growth factor as a novel strategy in treating lung cancer. Mol Canc Therapeut 2009;8:1106–12.
[28] Li SZ, Zhao YB, Cao WD, Qu Y, Luo P, Zhen HN, et al. The expression of hepatoma-derived growth factor in primary central; nervous system lymphoma and its correlation with angiogenesis; proliferation and clinical outcome. Med Oncol 2013;30:1–7.
[29] Ke Y, Zhao W, Xiong J, Cao R. Downregulation of miR-16 promotes growth and motility by targeting HDGF in non-small cell lung cancer cells. FEBS Lett 2013;587:3153–7.
[30] Uyama H, Tomita Y, Nakamura H, Nakamori S, Zhang B, Hoshida Y, et al. Hepatoma-derived growth factor is a novel prognostic factor for patients with pancreatic cancer. Gastroenterology 2006;134:6043-8.
[31] Yoshida K, Tomita Y, Okuda Y, Yamamoto S, Enomoto H, Uyama H, et al. Hepatoma-derived growth factor is a novel prognostic factor for hepatocellular carcinoma. Ann Surg Oncol 2006;13:159–67.
[32] Zhou Y, Zhou N, Fang W, Huo J. Overexpressed HDGF as an independent prognostic factor is involved in poor prognosis in Chinese patients with liver cancer. Diagn Pathol 2010;5:58.
[33] Tsai CC, Huang SC, Tai MH, Chien CC, Huang CC, Hsu YC. Hepatoma-derived growth factor upregulation is correlated with prognostic factors of early-stage cervical adenocarcinoma. Int J Mol Sci 2014;15:21492–504.
[34] Zhao WY, Wang Y, An ZJ, Shi CG, Zhu GA, Wang B, et al. Downregulation of miR-497 promotes tumor growth and angiogenesis by targeting HDGF in non-small cell lung cancer. Biochem Biophys Res Commun 2013;435:466–71.
[35] Chen B, Huang T, Jiang J, Lv L, Li H, Xia S. miR-141 suppresses proliferation and motility of gastric cancer cells by targeting HDGF. Mol Cell Biochem 2014;388:211–8.